

Robotic Systems for Pavement Lane Painting Operations

Sangkyun Woo, Daehie Hong, Woo-Chang Lee, and Tae-Hyung Kim

Abstract—This paper deals with fully automating the pavement lane painting operations utilizing robotic technology. This study includes a novel design of robot structure that can be easily installed on support commercial truck and image processing algorithms that can recognize deteriorated lane marks. With this robot system, a single operator within a cab is capable of tracking the existing faded lane mark and performing re-painting operations on-site, so that the dangerous and time consuming manual operations can be eliminated. The feasibility of the developed robot was explored through the experiments with image data acquired from real pavement surface.

Index Terms— Construction Robots, Kalman Filter, Lane Mark, Lane Painting Robot

I. INTRODUCTION

THE main function of traffic lanes is to direct traffic flow safely and efficiently. They provide drivers with safe driving condition. The pavement lanes must be frequently re-painted in order to keep the safe condition and prevent traffic accidents. However, current lane painting operations are manually carried out by several workers in most countries, which is very slow and labor-intensive. The manual operations require blocking traffic for a long period of time and bring serious traffic jam. In addition, the manual operations are potentially dangerous to the workers because they are exposed to passing traffic. Nowadays, robotic technologies are being actively utilized to automate many of construction tasks. The lane painting operations can be also automated with cutting-edge robotic technologies, which will bring dramatic reduction of working time, worker's safety, minimization of traffic blocking and accidents, and cost effectiveness.

The processes for automating the lane painting operations can be divided in two parts, lane recognition system and robotic

mechanisms to appropriately spray paint. There have been few efforts in this research area of robotic lane painting. Kotani et. al reported an image processing and motion control algorithm for lane mark drawing robot [1][2]. They used camera to detect lane mark and built prototype mobile robot to follow and re-paint the detected lane mark. Their system was very slow due to the limitations on image processing hardware and software. Paint nozzle was fixed to the robot body, so that the control for tracking the existing lane mark was achieved by moving robot body. This could make it difficult to realize fast and precise lane tracking in authors' view point. Koçekali and Ravani derived a path planning algorithm for stenciling robot of roadway marking [3]. They developed very big articulated robot system for the stenciling operations. This work did not include the lane marking operations.

In terms of the research on lane recognition, there have been many papers in the field of autonomous driving system. The lane mark recognition algorithms can be divided into two categories, which are inter-frame processing and intra-frame processing [4]. The inter-frame processing is a three dimensional lane geometry recognition [5]. It is very difficult to reliably extract necessary features from image information due to inconsistent lighting and road conditions, such as shadow, tire mark, line occlusion, etc. Jeong et al. used a Sobel operator among the differential operators to detect lane image [6], which has smooth effect as well as making the difference of image brightness conspicuously. Also, a concept of "model-based approach" has been frequently used to improve robustness [7]. The model is mathematical representations of lane structure and vehicle positions relative to the lane. Lane boundaries on the image are predicted through contrasting the real image with model projection. Dickmanns and Mysliwetz proposed method using Kalman filter with a model based approach [8]. The lane recognition algorithms developed for autonomous driving system mentioned herein have the potential to be utilized for the autonomous lane marking robot.

This paper deals with fully automating the pavement lane painting operations utilizing robotic technology. This study includes a novel design of robot structure that can be easily installed on support commercial truck and the image processing algorithm that can recognize half-faded lane mark. With this robot system, a single operator within a cab is capable of tracking the existing faded lane mark and performing re-painting operations on-site, so that the dangerous and time consuming manual operations can be eliminated.

The authors greatly acknowledge the KICTTEP for the support of this work through the project no. A-07 (Development of Roadway Sign Painting Robot System).

S. Woo is with Korea University, Seoul 136-701, Korea (e-mail: wwookane@korea.ac.kr).

D. Hong is with the Department of Mechanical Engineering, Korea University, Seoul 136-701, Korea (corresponding author to provide phone: 82-23290-3369; fax: 82-2-926-9290; e-mail: dhhong@korea.ac.kr).

W.-C. Lee was with Korea University. He is currently with Korean Navy, Taejeon, Korea (e-mail: nlwc@freechal.com).

T.-H. Kim is with the Korea Institute of Construction Technology, Kyungki-do, Korea (e-mail: tckim@kict.re.kr).

II. DESIGN OF LANE PAINTING ROBOT

The lane painting robot system consists of vision system and robot spray system. The vision system is to extract the lane feature from the original roadway image that is acquired by a CCD (Charge Coupled Device) camera. The robot spray system is to carry out actual tracking control and painting action by using the information from the vision system. Fig. 1 shows the block diagram of the proposed lane painting robot system. The vision system generates the positions of lane center and sends them to the robot control system. The robot is one-dimensional translational mechanism as shown in Fig. 2. The robot is designed to be installed under the left and/or right side of a truck bed. Most of current manual machines have fixed nozzle at the same location, so that the robot is intended to retrofit the existing manual machines. The paint nozzle head travels transversely to the lane direction, while the vehicle equipped with the robot system and supporting tools is running along the lane with high speed. The robot system is designed to be operated at the maximum speed of 20 km/h. Fig. 2 shows the one-dimensional robot and paint nozzle assembly. The paint nozzle is equipped with solenoid valve for automatic on/off control of paint flow from the control computer.

III. LANE RECOGNITION

A. Image Processing

The roadway surface image is acquired with CCD camera and frame grabber that is housed in a control computer. Then, the lane feature is extracted from the original image. The original image acquired from the camera is enhanced by using noise filter, in preprocessing step. In this step, low pass filter was used for eliminating noise from original image.

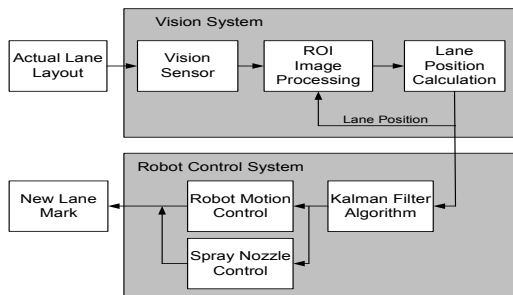


Fig. 1. Block diagram of the lane painting robot system.

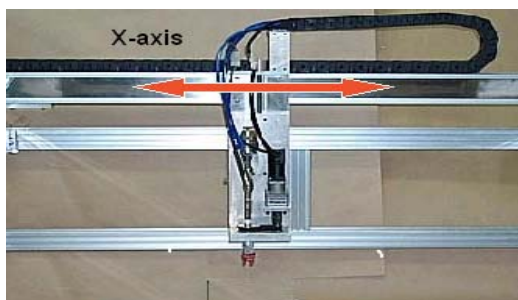


Fig. 2. Picture of robot and paint nozzle assembly.

Image processing is an operation dealing with the pixel values of an image. The image processing time is the most important factor in evaluating its performance and it is strongly related to the number of pixels for calculation. Thus, it is necessary for the system to reduce the number of pixels for real time operation. For this purpose, the region of interest (ROI) concept is very useful. The lane image occupies about 20 percent in the full size of roadway image. The number of pixels for calculation can be reduced in great amount by setting ROI based on the lane position that is estimated in the previous step. There exist many image processing algorithms that can be applied to the lane feature extraction. Edge detection method was chosen after carefully investigating some other image processing algorithms. The main limitation is calculation time for high speed lane painting. An edge is a significant local change in the image intensity, usually associated with a discontinuity in either the image intensity or the first and second derivatives of the image intensity.

Sobel operator is a differential operator which can efficiently remove most of useless information in the road image. The discrete Sobel operator is defined as following

$$\nabla_x f(x,y) = [f(x-1,y+1) + 2f(x,y+1) + f(x+1,y+1)] - [f(x-1,y-1) + 2f(x,y-1) + f(x+1,y-1)] \quad (1)$$

$$\nabla_y f(x,y) = [f(x-1,y-1) + 2f(x-1,y) + f(x-1,y+1)] - [f(x+1,y-1) + 2f(x+1,y) + f(x+1,y+1)] \quad (2)$$

The intensity gradient is defined as,

$$G(x,y) = \sqrt{\nabla_x f^2 + \nabla_y f^2} \quad (3)$$

Also, the tangent which indicates the direction of the intensity gradient is defined as,

$$\tan \alpha = \frac{\nabla_y f(x,y)}{\nabla_x f(x,y)} \quad (4)$$

Sobel operator enhances the intensity difference between the processed point and its neighborhood. For normal road surface, the gray intensity values of the adjacent points are very close and they show big difference at the edge of lane feature. Fig. 3 shows an example of the image processing effect of edge enhancement with severely faded lane image.

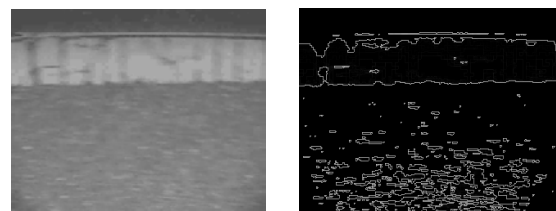


Fig. 3. Example of lane edge detection by Sobel operation.

The feature point extraction is an operation of searching relevant pixels in ROI. An optimum feature point is determined only one in one ROI. In the case that the relevant pixels are not selected, the ROI is extended to scan more pixels. Fig. 4 and the followings explain three possible cases of selecting the feature points that can happen in general faded lane mark:

Case 1: The width between the detected edges is too narrow due to the erased hole at the side of lane mark. If the detected width is less than 70% of nominal lane width (it is usually 15 cm according to the standard), this case is rejected to prevent hunting motion of the robot.

Case 2: This is the most ideal case where concurrent edges at both sides of lane mark are obtained without holes inside. The feature point can then be determined as a median value of the two effective edges.

Case 3: There exists at least one erased hole inside the lane mark. In this case, the inside edges are discarded and the far outside edges (points 1 and 4 in Fig. 4) are averaged to obtain the centerline of the lane mark.

Fig. 5 shows the screen of the image processing program built for the lane center extraction.

B. Lane Model and Kalman Filter

The line that is formed by connecting the center points obtained from the vision processing is not smooth mainly due to the faded lane mark images and also due to the vision sensor

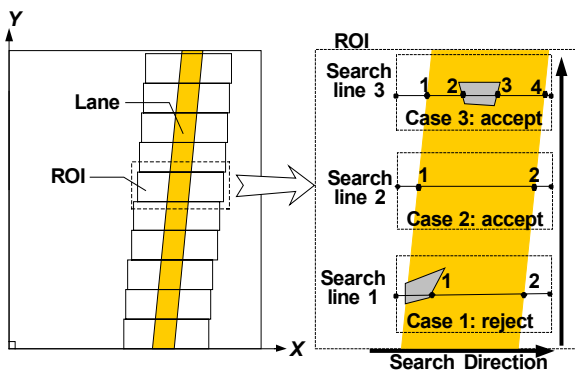


Fig. 4. Extraction processes of lane centers

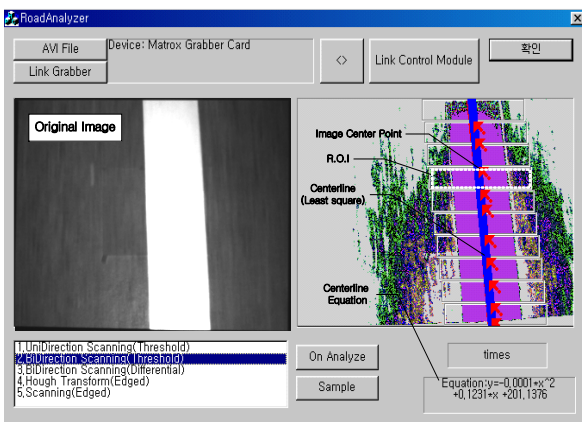


Fig. 5. Image processing program for lane center extraction.

noise. In order to solve this problem, the second order polynomial model is introduced for the centerline of the lane mark and Kalman filter is applied to smooth out the noisy data. The second order polynomial lane model characterizes constant curvature while the vehicle moves forward as can be seen in the following description. The Kalman filter is a recursive data processor which estimates the most probable state of a system utilizing, knowledge of system dynamics, measurements, assumed statistics of system noise and measurement errors, and initial condition information. The purpose of using Kalman filter is to produce optimal estimates of the state of a dynamic system on the basis of noisy measurements and an uncertain model of the system's dynamics. Kalman filter optimizes the measured sensor data that contains Gaussian white noise based on the constant curvature lane dynamics. In fact, the lane curvature is not constant all over the road but the curvature measured in the small area can be assumed constant. The view area of this system is about 1 square meters.

The lane model represented by the second order polynomial can be expressed as (5) [9]. Fig. 6 shows the vehicle fixed coordinate system that is defined according to the standard vehicle dynamics coordinate system [10].

$$y = c_0 + c_1x + c_2x^2 / 2 \tag{5}$$

According to the variation of the vehicle motion and the road shape, the coefficients of the polynomial vary dynamically. This polynomial can be expressed as nonlinear equations (6) and (7).

$$\dot{c}_0 = \frac{uc_0}{\cos c_1} - v \tag{6}$$

$$\dot{c}_1 = \frac{uc_2}{\cos c_1} - \omega \tag{7}$$

where u , v , ω are vehicle's forward, lateral, and yawing velocities, respectively.

Assuming that the curvature of the lane is constant and the heading angle is small, these equations can be expressed as a linear form, such that

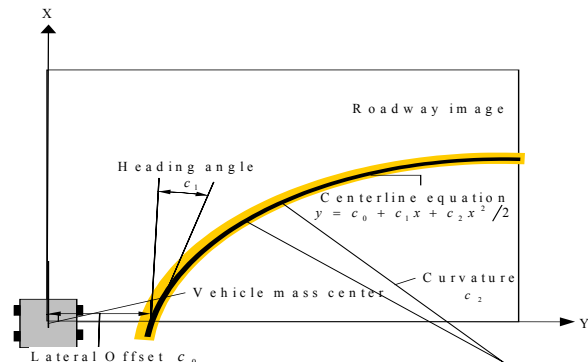


Fig. 6. Lane modeling with the 2nd order polynomial.

$$\begin{bmatrix} \dot{c}_0 \\ \dot{c}_1 \\ \dot{c}_2 \end{bmatrix} = \begin{bmatrix} 0 & u & 0 \\ 0 & 0 & u \\ 0 & 0 & 0 \end{bmatrix} \begin{bmatrix} c_0 \\ c_1 \\ c_2 \end{bmatrix} + \begin{bmatrix} -1 & 0 \\ 0 & -1 \\ 0 & 0 \end{bmatrix} \begin{bmatrix} v \\ \omega \end{bmatrix} \quad (8)$$

since $\cos c_1 \cong 1$ for small angle like $0 \leq c_1 \leq 15^\circ$, which is adequate to the most of lane followings for painting operations.

Equation (8) is then discretized for applying to Kalman filter with the following matrices and vectors,

$$\Phi = \begin{bmatrix} 1 & u & 0 \\ 0 & 1 & u \\ 0 & 0 & 1 \end{bmatrix}, \mathbf{C} = \begin{bmatrix} c_0 \\ c_1 \\ c_2 \end{bmatrix}, \mathbf{\Gamma} = \begin{bmatrix} -1 & 0 \\ 0 & -1 \\ 0 & 0 \end{bmatrix}, \mathbf{u} = \begin{bmatrix} v \\ \omega \end{bmatrix} \quad (9)$$

and the measurement and noise vectors are represented as:

$$\begin{aligned} \mathbf{Y}_k &= \mathbf{H}\mathbf{C}_k + w_k \\ w_k &\sim \mathbf{N}(\mathbf{0}, \mathbf{Q}_k) \end{aligned} \quad (10)$$

where the coefficient matrix is

$$\mathbf{H} = \begin{bmatrix} 1 & x_1 & x_1^2/2 \\ 1 & x_2 & x_2^2/2 \\ \cdot & \cdot & \cdot \\ 1 & x_9 & x_9^2/2 \\ 1 & x_{10} & x_{10}^2/2 \end{bmatrix} \quad (11)$$

Then, the Kalman filter consists of the following 5 equations,

$$\hat{\mathbf{C}}_k(-) = \Phi \mathbf{C}_{k-1}(+) + \mathbf{\Gamma} \mathbf{u}_{k-1} \quad (12)$$

$$\hat{\mathbf{C}}_k(+) = \mathbf{C}_k(-) + \mathbf{K}_k (\mathbf{Y}_k - \mathbf{H} \hat{\mathbf{C}}_k(-)) \quad (13)$$

$$\mathbf{P}_k(-) = \Phi \mathbf{P}_{k-1}(+) \Phi^T + \mathbf{Q}_k \quad (14)$$

$$\mathbf{K}_k = \mathbf{P}_k(-) \mathbf{H}^T [\mathbf{H} \mathbf{P}_k(-) \mathbf{H}^T + \mathbf{R}_k]^{-1} \quad (15)$$

$$\mathbf{P}_k(+) = [\mathbf{I} - \mathbf{K}_k \mathbf{H}] \mathbf{P}_k(-) \quad (16)$$

The Kalman filter gains and the state variables are estimated through the successive calculations of (12)-(16). For the existing lane mark that is severely faded away, the Kalman filter gives optimal center location of the lane mark based on its kinematics and noise statistics.

IV. RESULTS AND DISCUSSIONS

Fig. 7 shows the laboratory set-up for evaluating the performance of the lane painting robot system. In the experiments, input generator using computer graphics is utilized first for the performance analysis of the system. This

generator can mimic a real-road surface lane mark by adding noises in a curved solid line as shown in Fig. 8. A sinusoidal curve is used as an input. The basic width, period, and amplitude of sinusoidal inputs are 150 mm, 10000 mm, and 250 mm, respectively. The experimental conditions are different velocities (5, 10, 15, 20 km/h), different lanes (clean and noisy), and different algorithms (image processing only and Kalman filtering).

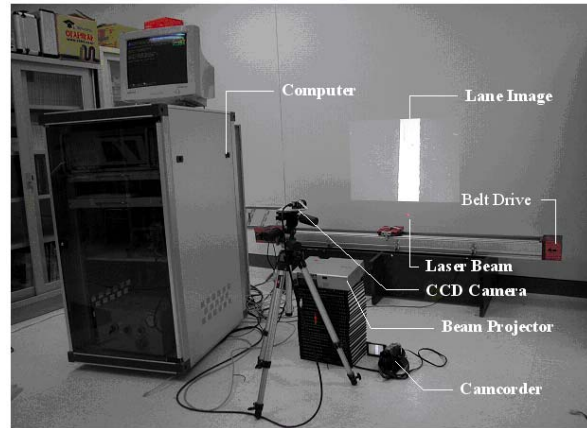


Fig. 7. Experimental set up for evaluating the proposed lane painting system

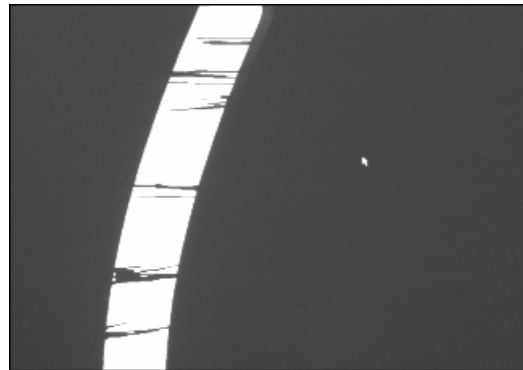


Fig. 8. An example of simulated lane input

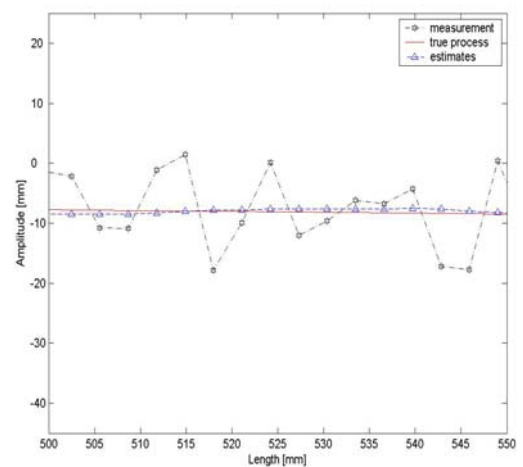


Fig. 9. Kalman filtering result

The experiments are divided into two steps. The first step is lane detection test to verify the lane detection performance with the comparative analysis between the simulation inputs and the outputs reconstructed from the inputs using image processing. The second step is lane tracking test to validate the lane tracking performance. In this step, the image processing result obtained from the first step is fed to the input of the robotic spray system, and this input is compared with the output of the robot system that is its position. Maximum errors (MAXE) and standard deviations (STD) of the errors are used as performance criteria. Table. I and Table. II show the lane detection and robot tracking performances. The Kalman filter outputs are appropriate even for noisy lane marks. Fig. 9 shows Kalman filter result for a part of lane mark.

TABLE I
EXPERIMENTAL RESULTS WITH SINUSOIDAL SIMULATION INPUT
(LANE DETECTION)

Velocity [km/h]	Noise	Image process	STD	MAXE [mm]
5	clean	applied	1.111	3.3
		not applied	2.012	6.3
	noisy	applied	1.308	5.2
		not applied	2.284	8.7
10	clean	applied	2.240	10.6
		not applied	3.329	15.3
	noisy	applied	3.246	13.4
		not applied	3.565	15.1
15	clean	applied	3.570	12.3
		not applied	5.468	15.4
	noisy	applied	4.741	14.8
		not applied	7.772	22.4
20	clean	applied	3.640	12.6
		not applied	7.923	18.9
	noisy	applied	3.423	10.7
		not applied	8.687	38.37



Fig. 10. An example picture of real load input

After the tests with simulated inputs, real images acquired from pavement surface with a digital camcorder were inputted to the image processing and robotic spray system. Fig. 10 shows a picture of lane recorded from real road surface. The experimental conditions are also different velocities (5, 10, 15, 20 km/h), different lane (clean and noisy) and different algorithm (image processing and Kalman filter). Table. III and Table. IV show the lane detection and robot tracking performances.

V. CONCLUSION

This paper presents a robotic system to automate pavement lane painting operations. The robot system consists of vision system to detect existing deteriorated lane marks and one dimensional actuator to position the paint spray on the detected lane mark. Sobel operation and Kalman filtering are utilized for the main image processing technique. The system performance was tested with simulation inputs and actual roadway inputs. The tests showed satisfactory results to be used for automatic lane painting. With this robot system, a single operator within a cab is capable of tracking the existing faded lane mark and performing re-painting operations on-site, so that the dangerous and time consuming manual operations can be eliminated.

TABLE II
EXPERIMENTAL RESULTS WITH SINUSOIDAL SIMULATION INPUT
(ROBOT TRACTING)

Velocity [km/h]	Noise	Kalman filtering	STD	MAXE [mm]
5	clean	applied	1.226	3.8
		not applied	1.723	5.5
	noisy	applied	1.876	7.2
		not applied	2.247	9.0
10	clean	applied	2.307	11.1
		not applied	2.688	13.9
	noisy	applied	3.217	12.8
		not applied	3.793	15.6
15	clean	applied	4.175	13.2
		not applied	5.023	15.5
	noisy	applied	5.476	17.2
		not applied	7.398	22.8
20	clean	applied	4.775	15.7
		not applied	6.944	19.2
	noisy	applied	4.236	10.1
		not applied	7.581	39.4

TABLE III
EXPERIMENTAL RESULTS WITH REAL LANE
(LANE DETECTION)

Velocity [km/h]	Noise	Image process	STD	MAXE [mm]
5	clean	applied	2.295	7.7
		not applied	6.138	14.4
	noisy	applied	1.996	6.1
		not applied	6.230	16.0
10	clean	applied	3.277	14.4
		not applied	6.58	21.7
	noisy	applied	4.965	17.7
		not applied	6.767	21.5
15	clean	applied	4.641	14.7
		not applied	7.943	22.7
	noisy	applied	4.887	16.0
		not applied	9.594	32.1
20	clean	applied	3.979	13.2
		not applied	9.816	26.2
	noisy	applied	3.748	10.4
		not applied	10.74	44.6

TABLE IV
EXPERIMENTAL RESULTS WITH REAL LANE
(ROBOT TRACTING)

Velocity [km/h]	Noise	Kalman filtering	STD	MAXE [mm]
5	clean	applied	2.484	7.1
		not applied	6.058	15.2
	noisy	applied	2.306	9.5
		not applied	6.290	16.2
10	clean	applied	3.737	13.2
		not applied	6.487	21.9
	noisy	applied	5.285	19.9
		not applied	6.767	24.5
15	clean	applied	5.498	17.1
		not applied	7.650	22.5
	noisy	applied	5.725	18.7
		not applied	9.401	28.8
20	clean	applied	5.354	18.7
		not applied	8.853	23.7
	noisy	applied	4.591	11.7
		not applied	9.937	33.4

REFERENCES

- [1] S. Kotani, S. Yasutomi, X. Kin, H. Mori, S. Shigihara, and Y. Matsumuro, "Image processing and motion control of a lane mark drawing robot," *International Conference on Intelligent Robots and Systems*, 1993, pp. 1035–1041.
- [2] S. Kotani, H. Mori, S. Shigihara, and Y. Matsumuro, "Development of a lane mark drawing robot," *Proceedings of the 1994 IEEE International Symposium on Industrial Electronics*, 1994, pp. 320–325.
- [3] H. Koçekali and B. Ravani, "Feature based path planning system for robotic stenciling of roadway markings," *ASCE Specialty Conference on Robotics for Challenging Environments*, 1994, pp. 52–60.
- [4] M. Aoki, "Image processing in ITS," *IEEE International Conference on Intelligent Vehicle*, 1998, pp. 255–267.
- [5] G. Y. Chen and W. H. Tsai, "Vision-based unsupervised learning of unexplored environment for autonomous land vehicle navigation," *IEEE International Conference on Intelligent Vehicle*, 1998, pp. 697–708.
- [6] S. G. Jeong, C. S. Kim, K. S. Yoon, J. N. Lee, and J. I. Bae, "Real-Time lane detection for autonomous navigation," *IEEE Intelligent Transportation System Conference Proceeding*, 2001, pp. 508–513.
- [7] A. Takahashi and Y. Ninomiya, "Model-based lane recognition," *IEEE International Conference on Intelligent Vehicle*, 1996, pp. 314–320.
- [8] E. D. Dickmanns and B.D. Mysliwetz, "Recursive 3-D road and relative ego-state recognition," *IEEE Computer Society Technical Committee on Pattern Analysis and Machine Intelligence*, 1992, pp. 199–213.
- [9] Y. J. Park and K. S. Huh, "Development of a lane sensing algorithm using vision sensors," *KSME (The Korean Society of Mechanical Engineering)*, 2002, pp. 1666–1671.
- [10] T. D. Gillespie, *Fundamental of vehicle dynamics*, Society of Automotive Engineers, Inc 1992.